Dynamics of immune effector mechanisms during infection with *Mycobacterium avium* in C57BL/6 mice

Markus Haug,[1,2] Jane A. Awuh,[1] Magnus Steigedal,[1,2] June Frengen Kojen,[1] Anne Marstad,[1] Ivar S. Nordrum,[3,4] Øyvind Halaas[1] and Trude H. Flo[1]

[1]*Department of Cancer Research and Molecular Medicine, Centre of Molecular Inflammation Research, NTNU, Trondheim,* [2]*St Olav's Hospital, Trondheim,* [3]*Department of Pathology and Medical Genetics, St Olav's Hospital, Trondheim, and* [4]*Department of Laboratory Medicine, Children's and Women's Health, NTNU, Trondheim, Norway*

doi:10.1111/imm.12131
Received 27 March 2013; revised 10 May 2013; accepted 03 June 2013.
Correspondence: Trude Helen Flo, Centre of Molecular Inflammation Research and Department of Cancer Research and Molecular Medicine, NTNU, Faculty of Medicine, PB 8905, N-7491 Trondheim, Norway.
Email: trude.flo@ntnu.no
Senior author: Trude Helen Flo

Summary

Opportunistic infections with non-tuberculous mycobacteria such as *Mycobacterium avium* are receiving renewed attention because of increased incidence and difficulties in treatment. As for other mycobacterial infections, a still poorly understood collaboration of different immune effector mechanisms is required to confer protective immunity. Here we have characterized the interplay of innate and adaptive immune effector mechanisms contributing to containment in a mouse infection model using virulent *M. avium* strain 104 in C57BL/6 mice. *M. avium* caused chronic infection in mice, as shown by sustained organ bacterial load. In the liver, bacteria were contained in granuloma-like structures that could be defined morphologically by expression of the antibacterial innate effector protein Lipocalin 2 in the adjoining hepatocytes and infiltrating neutrophils, possibly contributing to containment. Circulatory anti-mycobacterial antibodies steadily increased throughout infection and were primarily of the IgM isotype. Highest levels of interferon-γ were found in infected liver, spleen and serum of mice approximately 2 weeks post infection and coincided with a halt in organ bacterial growth. In contrast, expression of tumour necrosis factor was surprisingly low in spleen compared with liver. We did not detect interleukin-17 in infected organs or *M. avium*-specific T helper 17 cells, suggesting a minor role for T helper 17 cells in this model. A transient and relative decrease in regulatory T cell numbers was seen in spleens. This detailed characterization of *M. avium* infection in C57BL/6 mice may provide a basis for future studies aimed at gaining better insight into mechanisms leading to containment of infections with non-tuberculous mycobacteria.

Keywords: adaptive immune response; $CD4^+$ T cell subsets; inflammation; mouse infection model; *Mycobacterium avium*.

Introduction

Non-tuberculous mycobacteria are widespread in the environment and their pathogenicity is receiving increased attention. Members of the most common subgroup, *Mycobacterium avium* complex, cause disease in immunocompromised patients and individuals with predisposing lung abnormalities, but only occasionally in the healthy population (reviewed in refs 1–3). Previous lung infections such as tuberculosis and inflammatory disorders with pulmonary manifestations such as cystic fibrosis and rheumatoid arthritis can predispose a person to *M. avium* complex disease, in particular if patients are on immunosuppressive medications like anti-tumour necrosis factor (TNF) therapy.[4,5] Inhalation of *M. avium* manifests as pulmonary disease whereas gastrointestinal involvement results from swallowing the bacteria. The infection can subsequently lead to disseminated disease in HIV-infected

Abbreviations: CFU, colony-forming unit; IL, interleukin; IFN, interferon; Lcn2, lipocalin 2; Th, T helper; TNF, tumour necrosis factor; Treg, regulatory T cells

patients not on anti-retroviral therapy.[6–8] In addition, lymphadenitis is observed in children without any underlying immunodeficiency.[9,10] Today there are no vaccines to *M. avium* complex diseases, and recommended treatment regimens are lengthy, expensive and frequently show treatment failure or poor outcomes.[11,12] To discover new therapeutic targets and for rational vaccine design we need to improve our understanding of the molecular and cellular host defence mechanisms providing protective immunity towards non-tuberculous mycobacteria.

Like the more virulent *Mycobacterium tuberculosis*, *M. avium* exploits macrophages as its primary host cell and causes chronic infections in mice with development of tissue granulomas.[13] Studies in mouse models have confirmed the role of central defence mechanisms shared with other intracellular pathogens, but also found aspects that seem to be divergent for *M. avium*, such as resistance to nitric oxide-mediated killing.[14,15] Further complicating research is the fact that virulence and host responses to *M. avium* seem to be greatly influenced by the mycobacterial strain and morphotype, the mouse strain, and the route of infection (reviewed in refs 16,17).

Innate immune responses are important for bacterial destruction, but the chronic nature and the high incidence of both *M. tuberculosis* and *M. avium* infections in patients with AIDS who have low levels of $CD4^+$ T cells points to the importance of adaptive immune effectors. A central step in the response to *M. avium* is the activation of $CD4^+$ T helper 1 (Th1) cells producing effector cytokines such as interferon-γ (IFN-γ) and TNF.[18] Genetic susceptibility studies in humans have further revealed that defects in interleukin-12 (IL-12),[19] IFN-γ[20] or, more recently, interferon regulatory factor-8[21] increase the risk for disseminated non-tuberculous mycobacterial disease in humans (overview in ref. 1). Inflammatory cytokines influence the outcome of mycobacterial infection by affecting the macrophage bactericidal capacity (IFN-γ, TNF), granuloma formation and maintenance (TNF, IL-1), activation of Th1 responses (IL-12), recruitment of effector cells (IL-8), increased (IL-6) and decreased (IL-10) effector responses in target T cells and macrophages (reviewed in refs 17,22,23). In addition, a range of antibacterial proteins like lipocalin 2 (Lcn2), secretory leucocyte protease inhibitor (SLPI) and cathelicidins are induced in response to infection that will affect mycobacterial survival.[24–27]

For *M. tuberculosis* infections there is increasing evidence that successful mycobacterial immunity in addition to Th1 cells involves engagement of other T cell subsets[28] and B cells.[29] B cells may be involved in successful long-term control of mycobacterial infections by influencing cytokine production, bacillary containment and immunopathological progression of disease (reviewed in refs 29,30). The impact of non-Th1 mechanisms is still poorly investigated in mycobacterial immunity in general and for *M. avium* immunity in particular and may involve innate immune proteins, B cells, $CD8^+$ T cells, natural killer and natural killer T cells, $\gamma\delta$ T cells, as well as $CD4^+$ $CD25^+$ $FoxP3^+$ regulatory T (Treg) cells and IL-17-producing pro-inflammatory T helper 17 (Th17) cells.[17,24,31–34] The Th17 cells constitute a strongly pro-inflammatory subset of effector T cells producing cytokines such as IL-17, IL-21 and IL-22, and mediate neutrophil recruitment to the site of inflammation,[35] whereas Treg cells are potent regulators of the adaptive immune response, suppressing T cell proliferation and cytokine production.[36]

We here characterize in detail the pathogenesis and the host's immune effector response mechanisms in C57BL/6 mice with *M. avium* 104, a virulent strain originally isolated from an AIDS patient[37] that is fully sequenced[38] and transformable. The strain was chosen as it has been described as of intermediate virulence, establishing chronic infection in C57BL/6 mice, and discussed as suitable for testing the effectiveness of vaccine candidates.[39] The intraperitoneal route of infection resulted in a fast systemic spread of the pathogen and reproducible chronic and non-resolving infection in visceral organs with bacteria contained in granulomatous structures. Our results extend previous work by analysing inflammatory cytokine levels and the antibacterial protein Lcn2 in infected organs, as well as addressing the more recently discovered Th17 and Treg cells. These findings will therefore be valuable for understanding the biology of mycobacterial infections in general and *M. avium* infections in particular.

Materials and methods

Mouse infections

All protocols on animal work were approved by the Norwegian National Animal Research Authorities and were carried out in accordance with Norwegian and European regulations and guidelines. C57BL/6 mice were purchased from Taconic (Bomholt, Denmark). *In vivo* infection was achieved by intraperitoneal injection of log-phase mycobacteria ($0{\cdot}5 \times 10^7$ to $5{\cdot}0 \times 10^7$ bacteria/mouse) in 0·5 ml PBS. At different time-points after infection, mice were killed and spleen, liver and blood samples were collected aseptically. Groups of four or five age-matched and sex-matched mice were used for each time-point. Bacterial load was measured by plating serial dilutions of organ homogenates (spleen, liver, in some experiments lung) or heparinized blood on Middlebrook 7H10 agar plates (Difco/Becton Dickinson, Franklin Lakes, NJ).

Mycobacteria

Transformants of the virulent *M. avium* clone 104 expressing firefly luciferase and displaying a smooth, transparent morphotype were used in all experiments and are described elsewhere.[24] Mycobacteria were cultured in Middlebrook

7H9 medium (Difco/Becton Dickinson) supplemented with glycerol (Merck, Darmstadt, Germany)/Tween 80 (Sigma, St Louis, MO)/Middlebrook ADC Enrichment (Difco/Becton Dickinson).

Histopathology and immunohistochemistry

Organ samples were fixed in buffered formalin, processed through standard dehydration, clearing and placed in paraffin overnight, cut in 5-μm thick sections and stained with two histochemical stains: haematoxylin & eosin, which is a general tissue stain, and Ziehl–Neelsen stain to detect acid-fast bacilli using methylene blue as counterstain. For immunostaining, sections were deparaffinized and subject to antigen retrieval at pH 6, blocked and incubated overnight at 4° (TNF) or for 1 hr at room temperature (lipocalin 2; Lcn2) with antibodies against TNF (ab34674, 1 : 100; Abcam, Cambridge, UK) or Lcn2 (polyclonal rabbit anti-mouse Lcn2 antibody 807).[40] This was followed by incubation with biotinylated secondary antibody (goat-anti-rabbit, 1 : 200; Dako, Glostrup, Denmark) and LSAB2 streptavidin-horseradish peroxidase (Dako). Sections were resolved using the EnVision DAB dectection system (Dako).

Cytokine detection by ELISA and quantitative real-time PCR

Cytokines levels were quantified by ELISA analysis from plasma samples as well as homogenized liver and spleen tissue using ELISA kits for mouse IFN-γ ('Femto HS' Ready-SET-Go!; eBioscience, San Diego, CA) and TNF (TNF-α DuoSet; R&D Systems, Minneapolis, MN). For quantitative real-time PCR analysis, tissue samples from spleen and liver were homogenized by bead-beating with a FastPrep-24 instrument (MP Biomedicals, Solon, OH). Total RNA was isolated in an automated protocol using the RNeasy Mini Kit with DNase I digestion on a QIAcube instrument (all Qiagen, Hilden, Germany). After cDNA synthesis (High-Capacity Reverse Transcription Kit, Applied Biosystems, Foster City, CA), quantitative real-time PCR was performed on a StepOnePlus pPCR System using TaqMan Fast Advanced Master Mix and TaqMan Gene Expression Assays (all Applied Biosystems). Tissue samples from all mice in a group ($n = 4$ or $n = 5$) were pooled and run in duplicates. Gene expression was normalized to glyceraldehyde 3-phosphate dehydrogenase and β-actin as endogenous controls and relative quantification values to gene expression in uninfected mice were calculated with StepOne Software 2.1 (Applied Biosystems).

Mycobacteria-specific antibody responses

Specific antibody responses to *M. avium* were analysed in mouse serum samples by ELISA. Briefly, 96-well half-area ELISA plates (Corning, Incorporated Life Sciences, NY) were coated with culture filtrate from *M. avium* grown for approximately 10 days in Sauton's medium and filtered through a 0·22-μm sterile filter. Samples and standards were diluted in reagent buffer (0·1% Casein/0·1% BSA in PBS) and incubated at room temperature for 2 hr. Serial dilutions of Anti-*M. avium* complex Ab18104 (IgG1, QEDBioscience Inc., San Diego, CA) starting at 100 ng/ml was used as standard. Total mycobacteria-specific antibodies were detected by horseradish peroxidase-conjugated rabbit anti-mouse antibodies (Dako) diluted 1 : 2000 (30 min at room temperature), followed by tetramethylbenzidine Microwell Peroxidase Substrate System (KPL, Gaithersburg, MD). For determination of isotype distribution, mycobacteria-specific antibodies were detected by rabbit anti-mouse subclass-specific antibodies (Zymed, San Francisco, CA; 1 hr room temperature) followed by horseradish peroxidase-conjugated goat anti-rabbit antibodies (Dako) diluted 1 : 4000, and tetramethylbenzidine substrate. Absorbance was read at 450 nm subtracting 570 nm using a Wallac Victor Multilabel reader (PerkinElmer, Waltham, MA).

Isolation of splenocytes and flow cytometric characterization

After preparing single-cell suspensions and lysis of red blood cells (red blood cell lysis buffer, eBioscience), splenocytes were characterized for the expression of cell surface antigens by staining with monoclonal antibodies to CD4, CD8, CD19, CD25, CD44, CD45RB, CD69, T cell receptor α, T cell receptor $\gamma\delta$, CD11b, Ly-6G and F4/80 (eBioscience and BioLegend, San Diego, CA). Treg cells were detected by intracellular FoxP3 staining using a FoxP3 Fix/Perm kit (BioLegend) and FoxP3 antibody (clone 150D, BioLegend). Flow cytometric analysis was performed on a BD LSR II flow-cytometer (BD Biosciences). Absolute cell numbers of B and T cells per spleen were calculated from the relative frequencies using flow cytometric phenotyping and the total number of cells counted after isolation from the organ. Data were analysed using FlowJo software (Tree Star, Ashland, OR); statistical analysis was performed using GraphPad Prism (GraphPad Software, Inc., San Diego, CA).

Mycobacteria-specific T cell cytokine production

Isolated splenocytes were resuspended in RPMI-1640 (Sigma)/10% fetal calf serum/10 mM HEPES/50 μM 2-mercaptoethanol and 5×10^5 cells/well were seeded in 96-well tissue culture plates. Cells were incubated with *M. avium* overnight at a cell ratio of 1 : 1, Brefeldin A (eBioscience) was added for the last 4 hr. Unstimulated cells and cells stimulated with the T cell mitogen concanavalin A (2·5 μg/ml, Sigma) were used as controls. Cells were resuspended, surface-stained for CD4 and CD8 and

fixed with 2% paraformaldehyde. After permeablization with 0·05% saponin, intracellular cytokine-staining was performed with monoclonal antibodies to IFN-γ, TNF and IL-17 (eBioscience) and cells were analysed by flow cytometry.

Results

M. avium 104 causes chronic disseminated infection in C57BL/6 mice and is contained in non-necrotic granuloma-like structures in spleen and liver

C57BL/6 mice were infected intraperitoneally with the virulent *M. avium* strain 104 resulting in a rapid, systemic infection. Mycobacteria were found in the spleen, liver and blood 1 day after infection (Fig. 1a). Whereas the bacteria were gradually cleared from the blood, organ bacterial load increased for the first 10–20 days and then remained surprisingly constant in spleen, liver and lungs throughout the course of experiments (Fig. 1a,b) and was therefore classified as a chronic disseminated infection. In accordance with observations in mice[41,42] and humans,[43] the developing inflammatory response was reflected in splenomegaly peaking 20–30 days post infection with a sixfold to 10-fold increase in spleen weight (Fig. 1c). Splenomegaly seemed to be partly caused by growth or recruitment of cells as a twofold to threefold increase in total spleen cell numbers was found (Fig. 1d). Mice appeared surprisingly healthy throughout infection and showed no clinical signs of disease such as fever, weight loss, loss of appetite, ruffled fur or discomfort. We have followed mice for 25 weeks post infection without animals dying or fully clearing the infection (not shown).

A hallmark of infection with pathogenic mycobacteria is the formation of tissue granulomas around infected macrophages.[44] Granulomatous structures appeared in spleen and liver of *M. avium*-infected mice about 10 days post infection (Fig. 1e). In the spleen, granulomas evolved from ill-defined epitheloid structures with scattered multinucleated giant cells in the intervening red pulp (day 11), to more defined granulomas with only a few multinucleated giant cells (days 21 and 41). At day 98 the granulomas appeared to be less cellular, containing scattered elongated nuclei, and the number of multinucleated giant cells was markedly reduced. The fibrous central core of these late granulomas showed no sign of necrosis as observed in the study with *M. avium* strain 724R by Kondratieva *et al.*[45] Granulomas appeared mainly in the red pulp, and to a lesser extent in the follicles, either piercing the periphery or appearing inside. The number of liver granulomas increased along with the number of organ colony-forming units (Fig. 1f). From acid-fast staining we found mycobacteria in the liver and spleen almost exclusively localized to granulomas (Fig. 1g).

M. avium induces stronger inflammatory responses in liver than in spleen

Inflammatory proteins were in general more strongly induced in the liver than in the spleen, as seen for IL-1β and the NOD-like receptor protein 3 (NLRP3) inflammasome/caspase-1 involved in processing of IL-1β (Fig. 2a). Inducible nitric oxide synthase (iNOS; NOS2) was increasingly up-regulated in both spleen and liver (Fig. 2a). Both IFN-γ mRNA and protein peaked 12 days post infection in all studied organs followed by a decrease in plasma and the spleen, whereas liver levels were sustained (Fig. 2a–c). Interleukin-6 mRNA, important for T cell differentiation and early IFN-γ, appeared after IFN-γ induction (Fig. 2a). Surprisingly, TNF and IL-12 mRNA were only weakly induced in the spleen whereas a gradual increase over time was observed in the liver (Fig. 2a,b). We were unable to detect TNF protein in spleen and plasma while liver TNF was elevated throughout infection (Fig. 2c). Immunohistochemical staining revealed initial TNF production mostly in hepatocytes, although over time epitheloid, cytoplasm-rich cells (presumably macrophages) in liver granulomas stained increasingly positive for TNF (Fig. 2d). In contrast, only scattered epithelial cells made TNF in the spleen, until increased expression was seen in ill-defined granulomas at day 98 (Fig. 2d). Uninfected mice displayed no distinct staining of TNF in the spleen and only in a few liver cells (see Supplementary material, Fig. S1A).

We have previously shown that the inflammatory and bacteriostatic protein Lcn2 prevents the growth of extracellular *M. avium*.[24] Lcn2 protein and mRNA were strongly induced and sustained in spleen, liver and serum over the course of infection (Fig. 2a–c). Interestingly, immunohistochemical staining for Lcn2[40] revealed not only the presence of infiltrating neutrophils but also how inflammatory responses were first initiated in hepatocytes closely adjoining the granulomas (as indicated by the arrows in Fig. 2d) before progressing throughout the infected liver at later stages of infection. Actually, liver granulomas were easily identified as clusters of lymphocytes and mononuclear cells that do not make Lcn2 (Fig 2d and refs 40,46). In the spleen neutrophils were the most prominent Lcn2 producers, but the potent induction of Lcn2 mRNA (Fig. 2a,b) points to other cellular sources as well, because new synthesis is not induced in neutrophils.[47] Only scattered neutrophils stained positive for Lcn2 in uninfected mice (Fig. S1B).

Changes in splenic lymphocyte subsets during *M. avium* infection

A major source of inflammatory cytokines might be immune cells present in or attracted to the infected tissue. To assess the *M. avium*-specific immune effector

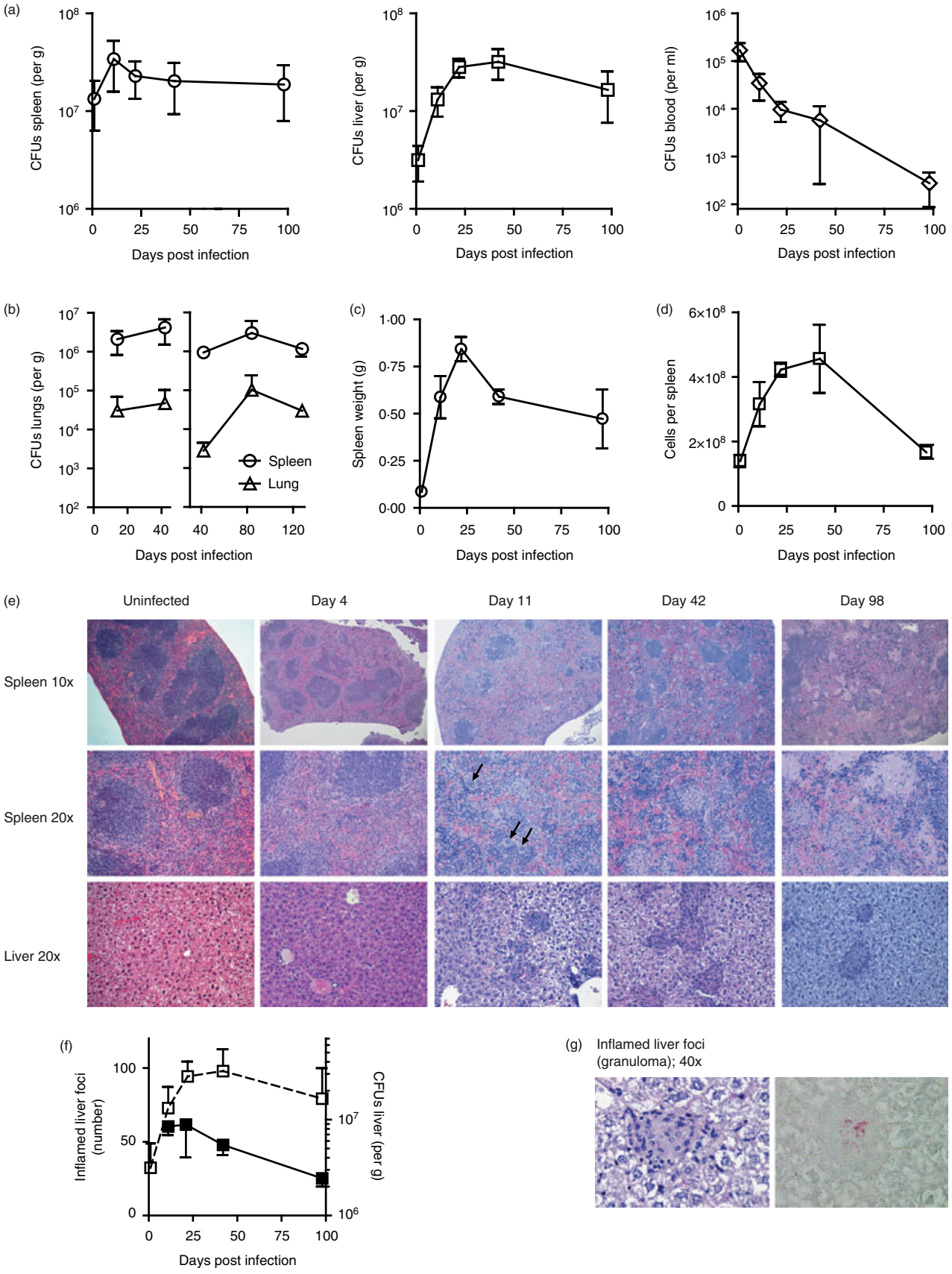
(a)
CFUs spleen (per g)
CFUs liver (per g)
CFUs blood (per ml)
Days post infection
(b)
CFUs lungs (per g)
Spleen
Lung
Days post infection
(c)
Spleen weight (g)
Days post infection
(d)
Cells per spleen
Days post infection
(e)
Uninfected
Day 4
Day 11
Day 42
Day 98
Spleen 10x
Spleen 20x
Liver 20x
(f)
Inflamed liver foci (number)
CFUs liver (per g)
Days post infection
(g)
Inflamed liver foci (granuloma); 40x

mechanisms at a cellular level we characterized the composition of spleen immune cell subsets at different times post infection. An example of flow cytometric analysis and gating of splenocytes is shown in Fig. 3(a). $CD19^+$ B cells and $CD3^+$ T cells constituted the majority of splenocytes. B cell numbers increased a few days after infection followed by an increase in T cell numbers around day 8 (Fig. 3b), and no loss of T cells was evident even at late time-points. T cell subtyping further revealed approximately 70% $CD4^+$ T cells and 25% $CD8^+$ T cells in the total $CD3^+$ T cell population at the initiation of infection, followed by a significant increase up to 38% $CD8^+$ T cells 20–30 days post infection (Fig. 3c, left graph). Of the $CD8^+$ T cells > 90% expressed the T cell receptor $\alpha\beta$ at the beginning of infection, increasing to 95% at day 30. In parallel we observed a decrease in relative T cell receptor $\gamma\delta$ expression (Fig. 3c, second graph). The fraction of naive T cells expressing an early activated phenotype ($CD44^{++}$ $CD69^+$) increased first for $CD4^+$ T cells (from around day 10) and later for $CD8^+$ T cells (Fig. 3c, third graph). Growing numbers of memory-type $CD4^+$ and $CD8^+$ T cells ($CD44^{++}$ $CD45RB^{low}$) were detected from day 17 (Fig. 3c, right), so with delayed kinetics compared with activated T cells ($CD44^{++}$ $CD69^+$, Fig. 3c, third graph). Relative frequencies and absolute numbers of B cells and different T cell subsets in the spleen can be found in Supplementary material, Table S1.

Mycobacterium-specific antibody production increases progressively during infection; $CD4^+$ and $CD8^+$ effector T cell responses coincide with reduced organ bacterial load

M.avium-specific antibodies were present in serum around day 10 (Fig. 3d, left graph), corresponding to the time when bacteria started to clear from the blood (as shown in Fig. 1a, right panel), and increasing concentrations of specific antibodies were observed over the 100-day experimental period (Fig. 3d). IgM was most abundant throughout infection and the isotype switch to IgG at later stages of infection (from day 42) was predominated by IgG2b antibodies followed by IgG2a and IgG3 (Fig. 3d, right graph).

Successful adaptive immunity towards *M. avium* depends on activation of mycobacteria-specific T cells producing effector cytokines.[18] The frequency of $CD4^+$ and $CD8^+$ T cells spontaneously producing IFN-γ was low in *M. avium*-infected spleens but could be increased by *in vitro* re-challenge with *M. avium* or the T cell-stimulating lectin concanavalin A (Fig. 3e, 23 days post infection). A subpopulation of the *M. avium*-specific, IFN-γ-producing $CD4^+$ effector T cells also produced TNF (about 10%, 1% of total $CD4^+$ T cells), but no sole TNF-producing $CD4^+$ T cells were found and $CD8^+$ T cells did not produce TNF in response to *M. avium* (Fig. 3e). An average of 0·63% of non-T cells in the spleen ($CD4^-$ and $CD8^-$ cells) yielded positive TNF-staining when stimulated with *M. avium* 23 days post infection, compared with 0·33% if the cells were not stimulated (not shown). Hence, only a very low number of non-T cells, such as macrophages, contributed to TNF production, pointing to $CD4^+$ T cells as the major source of TNF in the spleen. Isolated splenocytes from uninfected mice did not produce IFN-γ or TNF in response to *M. avium* (not shown).

Effector T cell responses were long-lasting; IFN-γ-producing $CD4^+$ as well as $CD8^+$ T cells were found in spleens throughout the infection (analysis up to 16 weeks post infection, Fig. 3f). *M.avium*-specific $CD4^+$ IFN-γ^+ Th1 cells appeared in the spleen as soon as 8 days post infection, followed by an abrupt onset of $CD8^+$ IFN-γ production on days 20–22 coinciding with reduced bacterial expansion (Fig. 3f), suggesting a role for *M. avium*-specific $CD8^+$ IFN-γ^+ T cell responses in restricting *M. avium* infection.

Infection with *M. avium* neither induces pro-inflammatory Th17 nor Treg cells

Pro-inflammatory Th17 cells and suppressive Treg cells represent more recently discovered $CD4^+$ T effector cell subsets whose role in mycobacterial infection has received

Figure 1. Course of long-term infection of *Mycobacterium avium* strain 104 in C57BL/6 mice. C57BL/6 mice were infected intraperitoneally with 5×10^7 colony-forming units (CFUs) *M. avium* and blood, spleen, liver and lungs analysed at different time-points post infection. (a) CFU counts in spleen (left), liver (middle) and peripheral blood (right). Results represent the mean and SD of CFUs/g organ or /ml blood of four or five mice at each time-point. (b) CFU counts in spleen and lung (data from two experiments different from the experiment shown in (a); procedures as described in (a). (c) Mean and SD of spleen weight at different time-points post infection. (d) Mean and SD of total cell numbers isolated from infected spleens at different time-points after infection. (e) Histopathology of the spleen (top and middle panel) and liver (lower panel) from uninfected mice and 4–98 days post infection [haematoxylin & eosin (H&E) staining, microscope objective 10× and 20×]. Examples of multinucleated giant cells are indicated with arrows (day 11, spleen, 20×). (f) Quantification of inflammatory foci (filled squares, left *y*-axis) compared with CFU counts (open squares, right *y*-axis) in livers from infected mice. Inflammatory foci were counted at different time-points from H&E stained liver histology samples and averaged from 10 fields of vision per organ (10×). (g) H&E (left) and Ziehl–Neelsen (right) staining of matching liver tissue sections 98 days post infection (40×). Acid-fast bacteria appear red with Ziehl–Neelsen staining. The results from one of three long-term infection experiments with similar outcomes are shown.

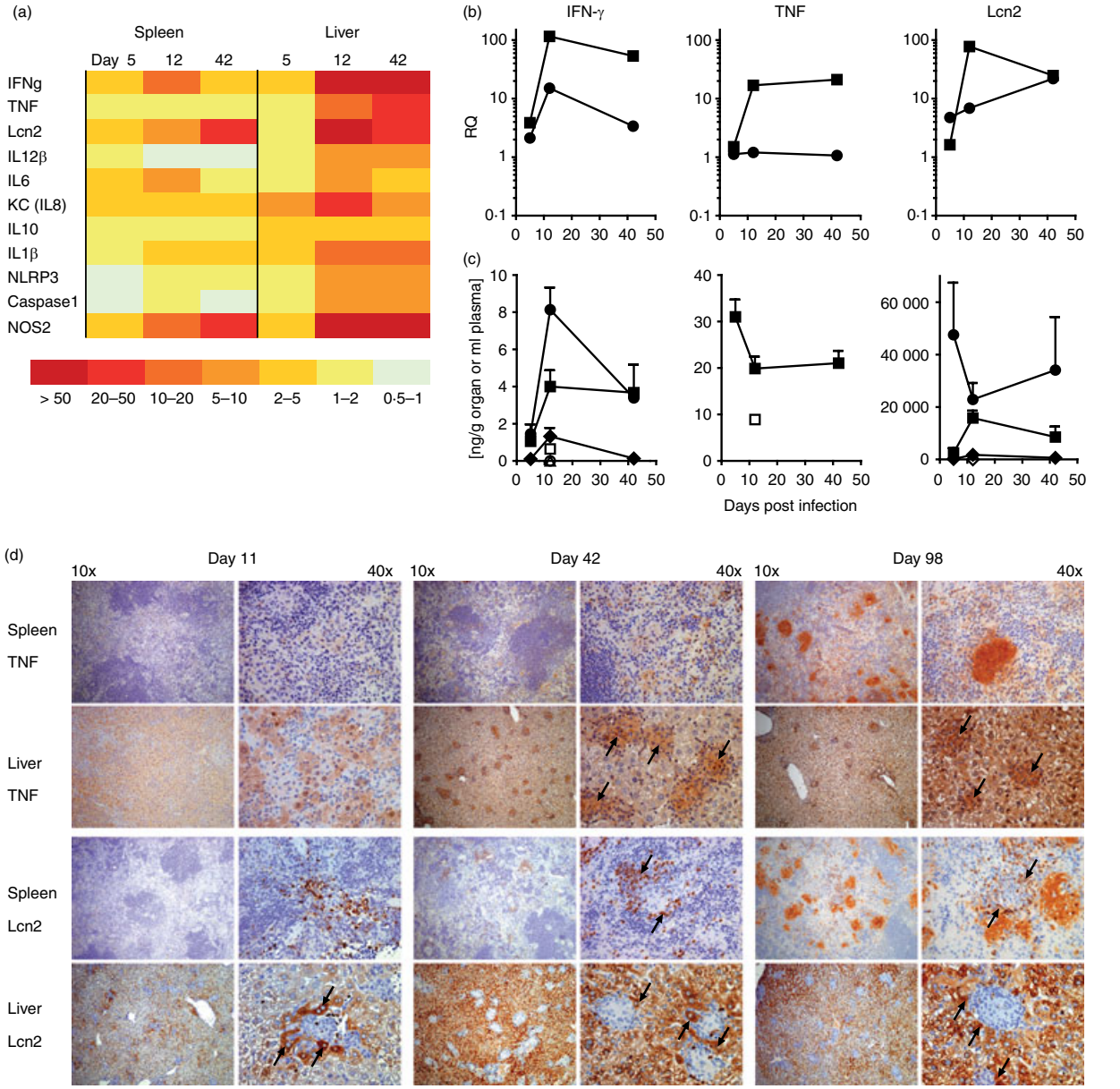

Figure 2. Inflammatory responses in infected organs and blood during long-term infection with *Mycobacterium avium* strain 104. C57BL/6 mice were infected with *M. avium* as described in Fig. 1 and selected host response parameters were analysed at different time-points post infection from spleen, liver and plasma samples. (a) Analysis of mRNA expression of inflammation-associated proteins interferon-γ (IFN-γ), tumour necrosis factor (TNF), lipocalin-2 (Lcn2), interleukin-12β (IL-12β), IL-6, KC (IL-8), IL-10, IL-1β, NOD-like receptor protein 3 (NLRP3), caspase-1 and inducible nitric oxide synthase (NOS2) in spleen and liver during *M. avium* infection by quantitative real-time PCR. Expression was analysed from pooled (n = 4 or n = 5 mice) spleen (left) and liver (right) homogenates 5, 12 and 42 days post infection and compared with uninfected controls. The results are displayed as a heat-map showing the relative changes in expression of selected genes during infection. (b) The relative mRNA expression data from (a) displayed as *xy*-diagram for IFN-γ (left), TNF (centre) and Lcn2 (right) in liver (closed squares) and spleen (closed circles). RQ = relative quantification of mRNA expression in infected versus uninfected mice. Results represent the mean and SD of triplicate measurements of pooled organ homogenates (n = 4 or n = 5 mice). (c) Expression of IFN-γ (left), TNF (centre) and Lcn2 (right) protein by ELISA [same experiment as in (a)]. Liver (squares) and spleen (circles) homogenates as well as plasma samples (diamonds) from infected (closed symbols) and uninfected (12 days post PBS injection, open symbols) mice were analysed. Results represent the mean and SD of triplicate measurements of pooled organ homogenates (n = 4 or n = 5 mice). (d) Immunohistochemical staining for TNF (upper two panels) and Lcn2 (lower two panels) of spleen and liver tissue on day 11 (left), 42 (centre) and 98 (right) post infection. Tissue samples are from the same experiment as in Fig. 1c; 10× and 40× magnification are shown. In the liver, hepatocytes and epitheloid cells were found to produce TNF, granuloma structures in the liver with TNF staining are indicated with arrows. Only scattered cells produced TNF in the spleen. High expression of Lcn2 was seen in liver and spleen, no Lcn2 was produced from cells inside the granuloma structures in liver but from hepatocytes closely adjoining the granulomas (indicated by arrows). Infiltrating neutrophils in the spleen stained strongly for Lcn2 (indicated by arrows).

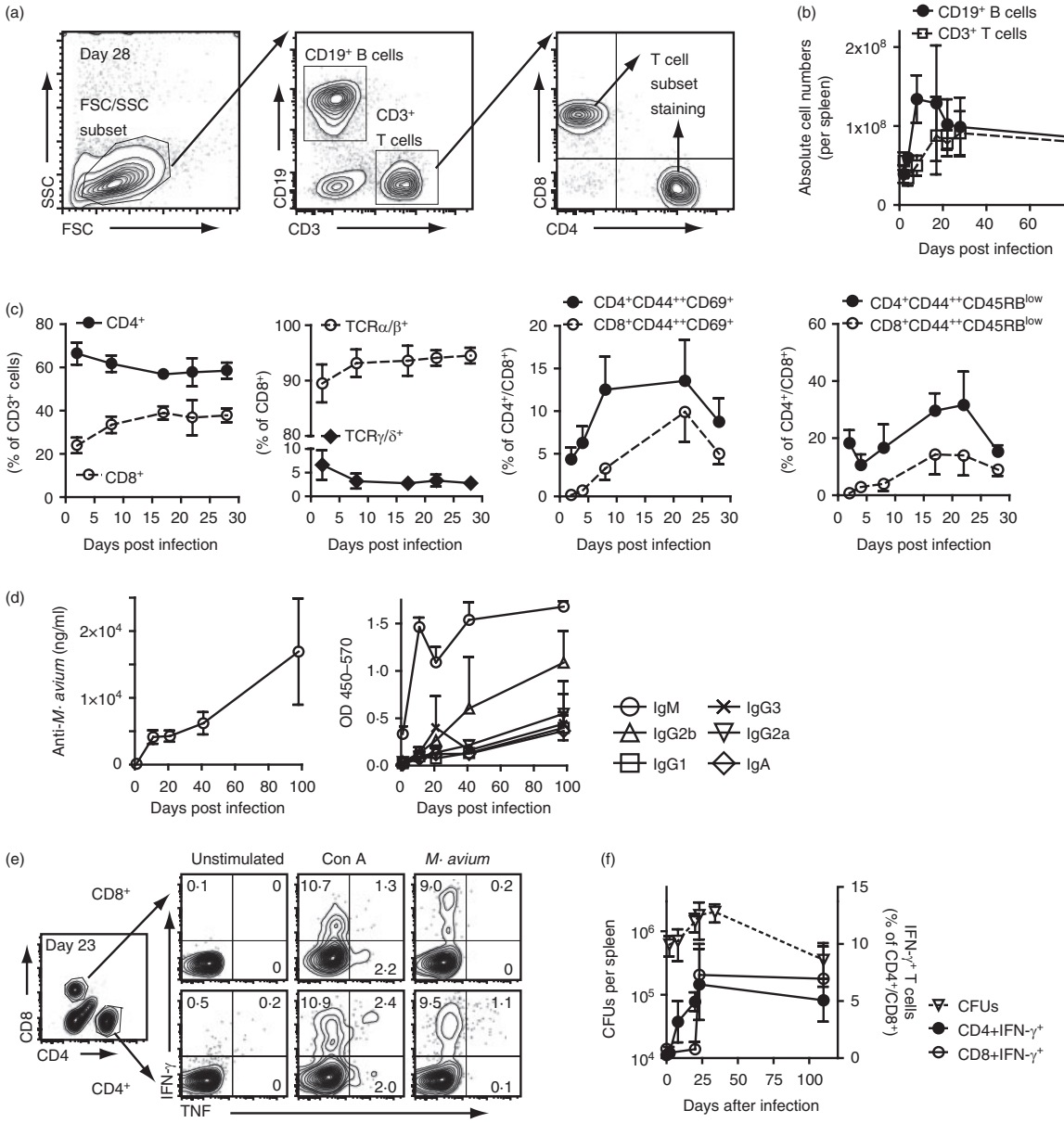

Figure 3. Development of adaptive B cell and T cell responses during long-term *Mycobacterium avium* strain 104 infection. Lymphocyte subsets were phenotyped from isolated spleen cells by flow cytometry at different time-points post *M. avium* infection. Results represent the mean and SD of four or five mice analysed at each time-point from one of four long-term infection experiments. (a) An example of flow cytometric gating and analysis of lymphocytes is shown (day 28 post infection). B cells ($CD19^+$) and T cells ($CD3^+$) were identified from the splenic lymphocyte population and sub-characterized by additional antibody staining. (b) Analysis of total numbers of spleen cells as well as B cell and T cell subsets. (c) Phenotyping of splenic T cell subsets during *M. avium* infection: Relative frequencies of $CD4^+$ and $CD8^+$ T cell subsets within the $CD3^+$ T cell population (left), T cell receptor usage (% of $CD8^+$ T cells expressing the $\alpha\beta$ or the $\gamma\delta$ T cell receptor, second from left), T cell subsets with an early activated phenotype (% of $CD44^{++}$ $CD69^+$ cells within the $CD4^+$ and $CD8^+$ T cell fraction, second from right, samples from day 17 were not analysed) and the subset of activated T cells developing a memory phenotype (% of $CD44^{++}$ $CD45RB^{low}$ cells within the $CD4^+$ and $CD8^+$ T cell fraction). (d) *M. avium*-specific antibodies in serum from infected mice at different time-points post infection. Left: Total antibody. Right: Isotype sub-characterization. Results represent the mean and SD of serum analysis of four or five mice at each time-point. (e) *M. avium*-specific T cell effector cytokine production in isolated splenocytes 23 days post infection. Interferon-γ (IFN-γ) (*y*-axis) and tumour necrosis factor (TNF) (*x*-axis) production of $CD8^+$ (upper panel) and $CD4^+$ (lower panel) T cells was analysed by intracellular cytokine-staining 20 hr after *in vitro* re-stimulation. Cytokine production from unstimulated cells (left), T cell mitogen concanavalin A (Con A, positive control, centre) and live *M. avium* (*M. avium* : splenocyte-ratio 1 : 1, right) stimulated cells were analysed. (f) Time–course of *M. avium*-specific IFN-γ effector cytokine production from $CD4^+$ and $CD8^+$ T cells during long-term infection. The $CD4^+$ and $CD8^+$ effector T cell frequencies are shown as an overlay with bacterial loads (CFUs) in spleens during long-term infection with *M. avium* strain 104. Results from one of four experiments with similar outcome are shown and represent the mean and SD of four or five mice analysed at each time-point.

increased research interest.[36,48–50] While different non-tuberculous mycobacteria were recently described to induce Th17 responses in humans[34] as well as bacillus Calmette–Guérin infection in IFN-γ-deficient mice,[49] Th17 and Treg cells have not been addressed in mouse *M. avium* infections.

We analysed Th17 cell frequencies by intracellular IL-17-staining of splenocytes at day 22 (not shown) and day 42 (Fig. 4a) post-*M. avium* infection. A tiny population of Th17 cells emerged when splenocytes were re-challenged with the positive control concanavalin A, but we did not detect IL-17-producing cells in response to *M. avium*. Moreover, no IL-17 messenger RNA could be measured in liver or spleen 5, 12 or 42 days post *M. avium* infection (not shown). The Treg cells were characterized as $CD4^+$ T cells co-expressing CD25 and the transcription factor FoxP3 ($CD4^+$ $CD25^+$ $FoxP3^+$, Fig. 4b). We observed a substantial relative decrease in splenic $FoxP3^+$ Treg cell numbers between days 10 and 20 post *M. avium* infection (Fig. 4c) coinciding with the increase in $CD44^+$ $CD69^+$ activated T cells (Fig. 3c), although no significant changes in total numbers of Treg cells were seen (Fig. 4d).

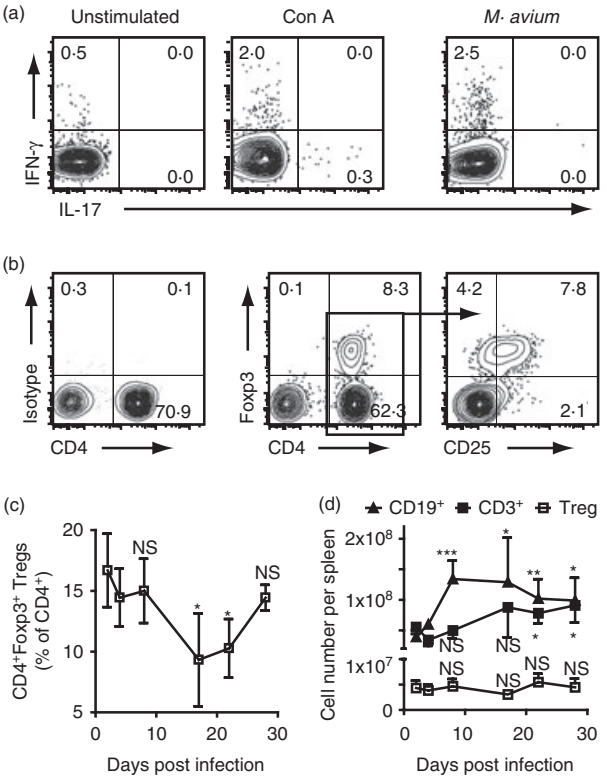

Figure 4. T helper type 17 (Th17) and T regulatory (Treg) cells during long-term infection with *Mycobacterium avium* strain 104. (a) *M. avium*-specific Th17 cells were analysed from production of the effector cytokine interleukin-17A (IL-17A). Spleen cells from infected mice were analysed by intracellular flow cytometry after *in vitro* re-stimulation as described in (c). One representative example for Th17 staining from a mouse 42 days post *M. avium* infection is shown. (b) Detection of $CD4^+$ T cells with a regulatory phenotype ($CD4^+$ $CD25^+$ $FoxP3^+$). $CD3^+$ gated T cells were characterized for $CD4^+$ and intracellular FoxP3 as well as CD25 expression. Intracellular staining with isotype-matched antibody to FoxP3 did not stain T cells (left). A subpopulation of $CD4^+$ T cells expressed $FoxP3^+$ (centre), the majority of these cells were in addition found to express CD25 (right). (c) Relative frequency of T cells with regulatory phenotype in spleens of mice during a 4-week *M. avium* infection. Relative frequencies reflect the fraction of $CD3^+$ $CD4^+$ $FoxP3^+$ cells as % within the total population of $CD3^+$ $CD4^+$ T cells; shown are data from one of more than three experiments with similar outcome; three to five infected mice per time-point; $^*P < 0{\cdot}05$ if compared with mice early after infection (day 2). (d) Absolute cell numbers of $CD19^+$ B cells, $CD3^+$ T cells and $CD3^+$ $CD4^+$ $FoxP3^+$ regulatory T cells per organ in spleens at different time-points during infection with *M. avium*. Absolute cell numbers were calculated from the relative frequencies and the total number of cells counted after isolation from the organ. Results from the same experiment as in (c) are shown; $^*P < 0{\cdot}05$, $^{**}P < 0{\cdot}01$, $^{***}P < 0{\cdot}001$ if compared with mice early after infection (day 2). Results represent the mean and SD of four or five mice analysed at each time-point.

Discussion

We still have an incomplete understanding of successful anti-mycobacterial immunity and mouse infection models are valuable to reveal cellular and molecular defence mechanisms relevant for anti-mycobacterial therapy. A central challenge in studying immune functions towards non-tuberculous mycobacteria such as *M. avium* is the huge variety of *M. avium* strains and their diversity. *Mycobacterium avium* isolates range from non-virulent with clearance of the infection[39,51] to highly virulent strains causing uncontrolled growth of the pathogen, T cell loss and induction of necrosis in granulomatous structures of infected mice.[52–54] In this study we have characterized the complex interplay of immune effector mechanisms in C57BL/6 mice during infection with the clinical isolate *M. avium* 104. The intraperitoneal route of infection was chosen as it reproducibly results in a rapid, systemic infection[24] that is sustained without resolution, similar to intravenous administration as shown by Saunders *et al.*[39] We confirm the results of Saunders *et al.* that *M. avium* 104 established chronic disseminated infection in tissues with inflammatory cell recruitment, granuloma formation as well as strong T cell responses,[39] and we extend the findings by characterizing additional cellular and molecular host defence mechanisms that may contribute to successful control of *M. avium* infection.

Expression of the innate immune effector protein Lcn2 dramatically increased both in serum and organs of infected mice. In the liver, bacteria were contained in granuloma-like structures that could be defined morphologically by expression of Lcn2 in adjoining hepatocytes and infiltrating neutrophils. Rodrigues *et al.*[55] also saw some Lcn2 induction around mycobacterium-positive

liver granulomas in a study where the authors suggest a possible role for Lcn2 in mycobacterium-induced anaemia. Lcn2 is also induced in mouse bone-marrow-derived macrophages,[24,40] but we could not detect Lcn2-producing macrophages or multinucleated giant cells in tissue granulomas. Takeda's group has demonstrated that Lcn2 is induced in alveolar macrophages and epithelial cells, and that Lcn2-deficient mice are susceptible to intratracheal infection with *M. tuberculosis*.[25] We have previously shown that Lcn2 prevents the growth only of extracellular *M. avium*,[24] but it is not possible to say if the massive induction of Lcn2 in hepatocytes along with release of pre-made Lcn2 from neutrophils could contribute to containment of the mycobacteria to granulomas.[47,56,57]

Like Lcn2, humoral immunity may also contribute to limit extracellular growth and spread of the mycobacteria.[29,30] Studies in mice and cynomolgus macaques infected with *M. tuberculosis* have demonstrated the presence in granulomas of activated B cells producing mycobacterium-specific antibodies,[58,59] and B cell deficient mice displayed exacerbated immunopathology and elevated lung bacterial burden compared with wild-types.[58] By comparing *M. avium* infections in BALB/c and SCID mice Fattorini *et al.*[31] have likewise suggested that both T and B cells are required to control *M. avium* infection. This is in line with our observations of elevated antibody production as well as IFN-γ^+ effector T cells throughout infection. A strong and early increase in B cell numbers and production of *M. avium*-specific antibodies from day 10 coincided with the early clearance of extracellular bacteria from the blood (day 10–20). The isotype dominance of IgM followed by IgG2b was slightly different from the IgG2a dominance described for *M. tuberculosis*-infected mice[60] and could reflect an abundance of lipids and sugars shed from the mycobacterial envelope promoting T cell independent IgM responses, but also the antigen coat used in the immunoassay (*M. avium* culture filtrate).

Through a series of studies by Bermudez, Appelberg, Ehlers and others, the individual roles of various inflammatory cytokines in *M. avium*-infected animals have been described.[13,17,18,61–64] As expected, the key effector cytokine IFN-γ mRNA and protein was sustained in infected organs throughout infection. TNF is, along with IFN-γ and IL-1, suggested to be important for granuloma development and containment of infection with *M. tuberculosis* and *M. avium*,[13,61,65] although the importance of TNF in mouse *M. avium* infection is not fully clarified. Ehlers *et al.*[62] found TNF receptor knock-out mice to be more susceptible to *M. avium* strain TMC724 infection as the result of deficiencies in granuloma formation, whereas Silva *et al.*[66] claimed a minor role for TNF especially with decreased virulence of the *M. avium* strain. In concordance with Appelberg *et al.*[18] we found low levels of TNF in *M. avium*-infected spleens. TNF mRNA was low and protein was undetectable (< 0·5 ng/g) in spleen homogenates, although we did observe some induction of TNF in inflamed areas of the spleen by immunohistochemistry but a fraction of isolated splenic CD4$^+$ T cells produced TNF in addition to IFN-γ. This finding indicates that mouse *M. avium* strain 104 infection results in induction of polyfunctional CD4$^+$ T cell responses with combined simultaneous production of several effector cytokines. The quality of CD4$^+$ and CD8$^+$ T cell responses, as measured by simultaneous production of IFN-γ, TNF and IL-2 from polyfunctional T cells, receives increased interest as it has been shown to correlate with protective long-term immunity against *M. tuberculosis*.[67] But although polyfunctional T cells were found to be important in vaccine-induced protection against pathogens such as *Leishmania major*,[68] polyfunctionality of the T cell responses alone seems not to be sufficient to predict protective vaccine immunity against *M. tuberculosis*.[69,70]

However, the low and local production of TNF may be sufficient, as formation of granuloma structures with containment of infection in the spleen was seen. Since bacterial containment in granuloma-like structure and control of infection was evident both in spleen and liver, our results suggest that TNF has a potent local effect in the spleen. It has been reported that less virulent mycobacteria are more sensitive to TNF.[71] We found adequate TNF responses in the liver as well as in isolated human or mouse macrophages (data not shown), so given the high influx of neutrophils and macrophages to the spleen from 1 week post infection we would have expected a higher production of inflammatory cytokines. Concomitant induction of anti-inflammatory IL-10 has previously been found to negatively influence the secretion of TNF and IFN-γ in response to mycobacterial infection compared with other Gram-positive or Gram-negative microbes in human peripheral blood monocytes.[34] However, we did not observe high inductions of IL-10 in the spleen and currently cannot explain the low levels of TNF and other inflammatory proteins induced by *M. avium* 104.

Different T cell subsets produce IL-17. The most prominent source is CD4$^+$ Th17 cells that seem more important in memory responses and vaccine-induced immunity than in control of primary *M. tuberculosis*.[49,72,73] Interleukin-17-producing $\gamma\delta$ T cells are also found in *M. tuberculosis*-infected tissue, although their function is rarely investigated.[74,75] We did not detect significant IL-17A expression in liver and spleen tissue, nor did we find *M. avium*-specific Th17 or increased numbers of $\gamma\delta$ T cells in spleens of infected mice. The absence of Th17 cell differentiation might possibly be a result of raised levels of IFN-γ, which has also been implicated as a negative regulator of antigen-specific Th17 development during primary bacillus Calmette–Guérin infection.[76] The decrease in relative $\gamma\delta$ T cell frequency might be explained by expansion of activated $\alpha\beta$ T cells as previously described in mouse *M. tuberculosis* infections.[74]

The role of regulatory T cells in mycobacterial infections is not yet clear and has been investigated mainly during early immune response in *M. tuberculosis* infections (reviewed in ref. 50). Data point to a role for Treg cells in delaying T cell priming in lymph nodes, but Treg cells are also present in infected tissue and granulomas. Little is known about the function of Treg cells in infections with *M. avium*, but HIV-infected patients with mycobacterial immune restoration disease seem to develop a strong Th1 response with functionally comprised Treg cells.[33] We observed no change in absolute splenic Treg cell numbers during the first 30 days of infection. This is in contrast to *M. tuberculosis*-infected mice, where the fraction of Treg cells was constant and so total numbers seemed to expand along with T cell numbers in affected organs.[77] However, we saw a relative decrease in Treg cell numbers between days 10 and 20 after infection coinciding with an increase in $CD44^+$ $CD69^+$ activated T cells and a strong pro-inflammatory cytokine environment in infected tissues. This phase favouring immune activation and inflammation rather than suppression might be important to successfully achieve containment of infection. Further studies of the function of Treg cells in non-tuberculous mycobacteria infections are ongoing.

The aim of this study was to provide a detailed characterization of the immune effector mechanism during *M. avium* strain 104 infection in C57BL/6 mice. The 104 strain was the first *M. avium* strain to be fully sequenced[38] and is suggested as a reference strain for testing the effectiveness of drug or vaccine candidates.[39] We think this model is useful also for *in vivo* studies of host–pathogen relations in mycobacterial infections because C57BL/6 is the most common genetic background for transgenic mice. Our study describes new aspects of innate, humoral and adaptive immune processes previously not addressed in the host's defence during long-term infections with *M. avium*. Together with studies revealing general mechanisms involved in mycobacterial infection[42] our findings may contribute to a better understanding of *M. avium* infections in particular and mycobacterial infections in general, and help in providing a solid basis for rational design of new vaccine and treatment strategies.

Acknowledgements

We thank Unn Granli and Eli Johansen at the Cellular and Molecular Imaging Core Facility, Faculty of Medicine, Norwegian University of Science and Technology (NTNU), and staff at the animal facility, Department of Comparative Medicine, NTNU and St Olav's hospital, for technical assistance in this project. The work was supported by the Liaison Committee between the Central Norway Regional Health Authority and the NTNU and the Research Council of Norway.

Disclosures

The authors have no conflicts of interests.

References

1 Reichenbach J, Rosenzweig S, Doffinger R, Dupuis S, Holland SM, Casanova JL. Mycobacterial diseases in primary immunodeficiencies. *Curr Opin Allergy Clin Immunol* 2001; **1**:503–11.
2 Wagner D, Young LS. Nontuberculous mycobacterial infections: a clinical review. *Infection* 2004; **32**:257–70.
3 Griffith DE. Nontuberculous mycobacterial lung disease. *Curr Opin Infect Dis* 2010; **23**:185–90.
4 Ehlers S. Why does tumor necrosis factor targeted therapy reactivate tuberculosis? *J Rheumatol Suppl* 2005; **74**:35–9.
5 Winthrop KL, Chang E, Yamashita S, Iademarco MF, LoBue PA. Nontuberculous mycobacteria infections and anti-tumor necrosis factor-α therapy. *Emerg Infect Dis* 2009; **15**:1556–61.
6 Jacobson MA, Hopewell PC, Yajko DM *et al.* Natural history of disseminated *Mycobacterium avium* complex infection in AIDS. *J Infect Dis* 1991; **164**:994–8.
7 Horsburgh CR Jr. *Mycobacterium avium* complex infection in the acquired immunodeficiency syndrome. *N Engl J Med* 1991; **324**:1332–8.
8 Horsburgh CR Jr, Gettings J, Alexander LN, Lennox JL. Disseminated *Mycobacterium avium* complex disease among patients infected with human immunodeficiency virus, 1985–2000. *Clin Infect Dis* 2001; **33**:1938–43.
9 Hazra R, Robson CD, Perez-Atayde AR, Husson RN. Lymphadenitis due to nontuberculous mycobacteria in children: presentation and response to therapy. *Clin Infect Dis* 1999; **28**:123–9.
10 Thegerstrom J, Romanus V, Friman V, Brudin L, Haemig PD, Olsen B. *Mycobacterium avium* lymphadenopathy among children, Sweden. *Emerg Infect Dis* 2008; **14**: 661–3.
11 van Ingen J, Egelund EF, Levin A *et al.* The pharmacokinetics and pharmacodynamics of pulmonary *Mycobacterium avium* complex disease treatment. *Am J Respir Crit Care Med* 2012; **186**:559–65.
12 Griffith DE, Aksamit TR. Therapy of refractory nontuberculous mycobacterial lung disease. *Curr Opin Infect Dis* 2012; **25**:218–27.
13 Hansch HC, Smith DA, Mielke ME, Hahn H, Bancroft GJ, Ehlers S. Mechanisms of granuloma formation in murine *Mycobacterium avium* infection: the contribution of $CD4^+$ T cells. *Int Immunol* 1996; **8**:1299–310.
14 Cooper AM, Pearl JE, Brooks JV, Ehlers S, Orme IM. Expression of the nitric oxide synthase 2 gene is not essential for early control of *Mycobacterium tuberculosis* in the murine lung. *Infect Immun* 2000; **68**:6879–82.
15 Gomes MS, Florido M, Pais TF, Appelberg R. Improved clearance of *Mycobacterium avium* upon disruption of the inducible nitric oxide synthase gene. *J Immunol* 1999; **162**:6734–9.
16 Cooper AM, Appelberg R, Orme IM. Immunopathogenesis of *Mycobacterium avium* infection. *Front Biosci* 1998; **3**:e141–8.
17 Appelberg R. Pathogenesis of *Mycobacterium avium* infection: typical responses to an atypical mycobacterium? *Immunol Res* 2006; **35**:179–90.
18 Appelberg R, Castro AG, Pedrosa J, Silva RA, Orme IM, Minoprio P. Role of γ interferon and tumor necrosis factor α during T-cell-independent and -dependent phases of *Mycobacterium avium* infection. *Infect Immun* 1994; **62**:3962–71.
19 Altare F, Durandy A, Lammas D *et al.* Impairment of mycobacterial immunity in human interleukin-12 receptor deficiency. *Science* 1998; **280**:1432–5.
20 Dorman SE, Picard C, Lammas D *et al.* Clinical features of dominant and recessive interferon γ receptor 1 deficiencies. *Lancet* 2004; **364**:2113–21.
21 Hambleton S, Salem S, Bustamante J *et al.* IRF8 mutations and human dendritic-cell immunodeficiency. *N Engl J Med* 2011; **365**:127–38.
22 Berrington WR, Hawn TR. *Mycobacterium tuberculosis*, macrophages, and the innate immune response: does common variation matter? *Immunol Rev* 2007; **219**:167–86.
23 Cooper AM, Mayer-Barber KD, Sher A. Role of innate cytokines in mycobacterial infection. *Mucosal Immunol* 2011; **4**:252–60.
24 Halaas O, Steigedal M, Haug M *et al.* Intracellular *Mycobacterium avium* intersect transferrin in the $Rab11^+$ recycling endocytic pathway and avoid lipocalin 2 trafficking to the lysosomal pathway. *J Infect Dis* 2010; **201**:783–92.
25 Saiga H, Nishimura J, Kuwata H *et al.* Lipocalin 2-dependent inhibition of mycobacterial growth in alveolar epithelium. *J Immunol* 2008; **181**:8521–7.
26 Nishimura J, Saiga H, Sato S *et al.* Potent antimycobacterial activity of mouse secretory leukocyte protease inhibitor. *J Immunol* 2008; **180**:4032–9.
27 Yuk JM, Shin DM, Lee HM *et al.* Vitamin D3 induces autophagy in human monocytes/macrophages via cathelicidin. *Cell Host Microbe* 2009; **6**:231–43.

28 Goldsack L, Kirman JR. Half-truths and selective memory: interferon γ, $CD4^+$ T cells and protective memory against tuberculosis. *Tuberculosis (Edinb)* 2007; **87**:465–73.

29 Maglione PJ, Chan J. How B cells shape the immune response against *Mycobacterium tuberculosis*. *Eur J Immunol* 2009; **39**:676–86.

30 Abebe F, Bjune G. The protective role of antibody responses during *Mycobacterium tuberculosis* infection. *Clin Exp Immunol* 2009; **157**:235–43.

31 Fattorini L, Mattei M, Placido R *et al. Mycobacterium avium* infection in BALB/c and SCID mice. *J Med Microbiol* 1999; **48**:577–83.

32 Chen ZW. Immune regulation of $\gamma\delta$ T cell responses in mycobacterial infections. *Clin Immunol* 2005; **116**:202–7.

33 Seddiki N, Sasson SC, Santner-Nanan B *et al.* Proliferation of weakly suppressive regulatory $CD4^+$ T cells is associated with over-active $CD4^+$ T-cell responses in HIV-positive patients with mycobacterial immune restoration disease. *Eur J Immunol* 2009; **39**:391–403.

34 Jonsson B, Ridell M, Wold AE. Non-tuberculous mycobacteria and their surface lipids efficiently induced IL-17 production in human T cells. *Microbes Infect* 2012; **14**:1186–95.

35 Kolls JK, Linden A. Interleukin-17 family members and inflammation. *Immunity* 2004; **21**:467–76.

36 Sakaguchi S, Miyara M, Costantino CM, Hafler DA. $FOXP3^+$ regulatory T cells in the human immune system. *Nat Rev Immunol* 2010; **10**:490–500.

37 Horan KL, Freeman R, Weigel K *et al.* Isolation of the genome sequence strain *Mycobacterium avium* 104 from multiple patients over a 17-year period. *J Clin Microbiol* 2006; **44**:783–9.

38 Semret M, Zhai G, Mostowy S *et al.* Extensive genomic polymorphism within *Mycobacterium avium*. *J Bacteriol* 2004; **186**:6332–4.

39 Saunders BM, Dane A, Briscoe H, Britton WJ. Characterization of immune responses during infection with *Mycobacterium avium* strains 100, 101 and the recently sequenced 104. *Immunol Cell Biol* 2002; **80**:544–9.

40 Flo TH, Smith KD, Sato S *et al.* Lipocalin 2 mediates an innate immune response to bacterial infection by sequestrating iron. *Nature* 2004; **432**:917–21.

41 Doherty TM, Sher A. Defects in cell-mediated immunity affect chronic, but not innate, resistance of mice to *Mycobacterium avium* infection. *J Immunol* 1997; **158**:4822–31.

42 Baldridge MT, King KY, Boles NC, Weksberg DC, Goodell MA. Quiescent haematopoietic stem cells are activated by IFN-γ in response to chronic infection. *Nature* 2010; **465**:793–7.

43 O'Reilly RA. Splenomegaly in 2,505 patients at a large university medical center from 1913 to 1995. 1963 to 1995: 449 patients. *West J Med* 1998; **169**:88–97.

44 Russell DG, Barry CE III, Flynn JL. Tuberculosis: what we don't know can, and does, hurt us. *Science* 2010; **328**:852–6.

45 Kondratieva E, Logunova N, Majorov K, Averbakh M, Apt A. Host genetics in granuloma formation: human-like lung pathology in mice with reciprocal genetic susceptibility to *M. tuberculosis* and *M. avium*. *PLoS One* 2010; **5**:e10515.

46 Berger T, Togawa A, Duncan GS *et al.* Lipocalin 2-deficient mice exhibit increased sensitivity to *Escherichia coli* infection but not to ischemia–reperfusion injury. *Proc Natl Acad Sci U S A* 2006; **103**:1834–9.

47 Kjeldsen L, Cowland JB, Borregaard N. Human neutrophil gelatinase-associated lipocalin and homologous proteins in rat and mouse. *Biochim Biophys Acta* 2000; **1482**:272–83.

48 Khader SA, Gopal R. IL-17 in protective immunity to intracellular pathogens. *Virulence* 2010; **1**:423–7.

49 Cruz A, Fraga AG, Fountain JJ *et al.* Pathological role of interleukin 17 in mice subjected to repeated BCG vaccination after infection with *Mycobacterium tuberculosis*. *J Exp Med* 2010; **207**:1609–16.

50 Urdahl KB, Shafiani S, Ernst JD. Initiation and regulation of T-cell responses in tuberculosis. *Mucosal Immunol* 2011; **4**:288–93.

51 Pedrosa J, Florido M, Kunze ZM *et al.* Characterization of the virulence of *Mycobacterium avium* complex (MAC) isolates in mice. *Clin Exp Immunol* 1994; **98**:210–6.

52 Benini J, Ehlers EM, Ehlers S. Different types of pulmonary granuloma necrosis in immunocompetent vs. TNFRp55-gene-deficient mice aerogenically infected with highly virulent *Mycobacterium avium*. *J Pathol* 1999; **189**:127–37.

53 Florido M, Cooper AM, Appelberg R. Immunological basis of the development of necrotic lesions following *Mycobacterium avium* infection. *Immunology* 2002; **106**:590–601.

54 Florido M, Goncalves AS, Silva RA, Ehlers S, Cooper AM, Appelberg R. Resistance of virulent *Mycobacterium avium* to γ interferon-mediated antimicrobial activity suggests additional signals for induction of mycobacteriostasis. *Infect Immun* 1999; **67**:3610–8.

55 Rodrigues PN, Gomes SS, Neves JV *et al. Mycobacteria*-induced anaemia revisited: a molecular approach reveals the involvement of NRAMP1 and lipocalin-2, but not of hepcidin. *Immunobiology* 2011; **216**:1127–34.

56 Appelberg R, Castro AG, Gomes S, Pedrosa J, Silva MT. Susceptibility of beige mice to *Mycobacterium avium*: role of neutrophils. *Infect Immun* 1995; **63**:3381–7.

57 Petrofsky M, Bermudez LE. Neutrophils from *Mycobacterium avium*-infected mice produce TNF-α, IL-12, and IL-1β and have a putative role in early host response. *Clin Immunol* 1999; **91**:354–8.

58 Maglione PJ, Xu J, Chan J. B cells moderate inflammatory progression and enhance bacterial containment upon pulmonary challenge with *Mycobacterium tuberculosis*. *J Immunol* 2007; **178**:7222–34.

59 Phuah JY, Mattila JT, Lin PL, Flynn JL. Activated B cells in the granulomas of nonhuman primates infected with *Mycobacterium tuberculosis*. *Am J Pathol* 2012; **181**:508–14.

60 Guirado E, Amat I, Gil O *et al.* Passive serum therapy with polyclonal antibodies against *Mycobacterium tuberculosis* protects against post-chemotherapy relapse of tuberculosis infection in SCID mice. *Microbes Infect* 2006; **8**:1252–9.

61 Smith D, Hansch H, Bancroft G, Ehlers S. T-cell-independent granuloma formation in response to *Mycobacterium avium*: role of tumour necrosis factor-α and interferon-γ. *Immunology* 1997; **92**:413–21.

62 Ehlers S, Benini J, Kutsch S, Endres R, Rietschel ET, Pfeffer K. Fatal granuloma necrosis without exacerbated mycobacterial growth in tumor necrosis factor receptor p55 gene-deficient mice intravenously infected with *Mycobacterium avium*. *Infect Immun* 1999; **67**:3571–9.

63 Bermudez LE, Young LS. Tumor necrosis factor, alone or in combination with IL-2, but not IFN-γ, is associated with macrophage killing of *Mycobacterium avium* complex. *J Immunol* 1988; **140**:3006–13.

64 Champsi JH, Bermudez LE, Young LS. The role of cytokines in mycobacterial infection. *Biotherapy* 1994; **7**:187–93.

65 Flynn JL, Goldstein MM, Chan J *et al.* Tumor necrosis factor-α is required in the protective immune response against *Mycobacterium tuberculosis* in mice. *Immunity* 1995; **2**:561–72.

66 Silva RA, Gomes MS, Appelberg R. Minor role played by type I tumour necrosis factor receptor in the control of *Mycobacterium avium* proliferation in infected mice. *Immunology* 2000; **99**:203–7.

67 Lindenstrom T, Agger EM, Korsholm KS *et al.* Tuberculosis subunit vaccination provides long-term protective immunity characterized by multifunctional CD4 memory T cells. *J Immunol* 2009; **182**:8047–55.

68 Darrah PA, Patel DT, De Luca PM *et al.* Multifunctional TH1 cells define a correlate of vaccine-mediated protection against *Leishmania major*. *Nat Med* 2007; **13**:843–50.

69 Kagina BM, Abel B, Scriba TJ *et al.* Specific T cell frequency and cytokine expression profile do not correlate with protection against tuberculosis after bacillus Calmette–Guérin vaccination of newborns. *Am J Respir Crit Care Med* 2010; **182**:1073–9.

70 Tameris MD, Hatherill M, Landry BS *et al.* Safety and efficacy of MVA85A, a new tuberculosis vaccine, in infants previously vaccinated with BCG: a randomised, placebo-controlled phase 2b trial. *Lancet* 2013; **381**:1021–8.

71 Sarmento AM, Appelberg R. Relationship between virulence of *Mycobacterium avium* strains and induction of tumor necrosis factor α production in infected mice and in *in vitro*-cultured mouse macrophages. *Infect Immun* 1995; **63**:3759–64.

72 Khader SA, Bell GK, Pearl JE *et al.* IL-23 and IL-17 in the establishment of protective pulmonary $CD4^+$ T cell responses after vaccination and during *Mycobacterium tuberculosis* challenge. *Nat Immunol* 2007; **8**:369–77.

73 Torrado E, Cooper AM. IL-17 and Th17 cells in tuberculosis. *Cytokine Growth Factor Rev* 2010; **21**:455–62.

74 Phyu S, Sornes S, Mustafa T, Tadesse A, Jonsson R, Bjune G. Changes in T-lymphocyte subsets in lungs and spleens of mice with slowly progressive primary *Mycobacterium tuberculosis* infection: involvement of unconventional T-cell subsets. *Scand J Immunol* 1999; **50**:137–44.

75 Lockhart E, Green AM, Flynn JL. IL-17 production is dominated by $\gamma\delta$ T cells rather than CD4 T cells during *Mycobacterium tuberculosis* infection. *J Immunol* 2006; **177**:4662–9.

76 Cruz A, Khader SA, Torrado E *et al.* Cutting edge: IFN-γ regulates the induction and expansion of IL-17-producing CD4 T cells during mycobacterial infection. *J Immunol* 2006; **177**:1416–20.

77 Scott-Browne JP, Shafiani S, Tucker-Heard G *et al.* Expansion and function of Foxp3-expressing T regulatory cells during tuberculosis. *J Exp Med* 2007; **204**:2159–69.

Supporting Information

Additional Supporting Information may be found in the online version of this article:

Figure S1. Staining controls immunohistochemistry.

Table S1. Characterization of B and T lymphocyte populations in spleens of *M. avium*-infected mice.

